SCIENCE CHINA
Technological Sciences

•Article•

October 2019 Vol.62 No.10: 1755–1759
https://doi.org/10.1007/s11431-018-9463-6

Oxygen vacancy and Mn^{2+} induced ferromagnetism in Mn-doped ZnO thin films

GUAN SuJun[1], NASU Naho[1], ZHANG Yu[2], TAMAMOTO Yuri[1], YAMANOBE Maria[1] & ZHAO XinWei[1,3*]

[1] *Department of Physics, Tokyo University of Science, Tokyo 162-8601, Japan;*
[2] *Department of Robotics, The Open University of Guangdong, Guangzhou 510091, China;*
[3] *Department of Materials Science and Engineering, Xihua University, Chengdu 610039, China*

Received November 23, 2018; accepted February 15, 2019; published online July 1, 2019

With the purpose of investigating the origin of ferromagnetism (FM), Mn-doped ZnO thin films had been fabricated by radio frequency (rf) magnetron sputtering and subsequent anneal process. The characterization of the Mn-doped ZnO thin films was conducted by X-ray diffraction (XRD), X-ray photoelectron spectroscopy (XPS), and superconducting quantum interference device (SQUID). With increasing the anneal temperature from 300°C to 700°C for 3 min, the influence on magnetism of the Mn-doped ZnO thin films is slight. While extending the anneal time from 3 to 50 min at 300°C, the influence on magnetism is obvious and the Mn-doped ZnO thin films with 30 min clearly demonstrate FM. Compared with the effect of oxygen vacancy and substitutional Mn^{2+} on the ferromagnetic behavior, O_V plays the main role in inducing FM of the Mn-doped ZnO thin films with good crystal structure.

oxygen vacancy, Mn^{2+}, ZnO, thin films, ferromagnetism

Citation: Guan S J, Nasu N, Zhang Y, et al. Oxygen vacancy and Mn^{2+} induced ferromagnetism in Mn-doped ZnO thin films. Sci China Tech Sci, 2019, 62: 1755–1759, https://doi.org/10.1007/s11431-018-9463-6

1 Introduction

The discovery of giant magnetoresistance makes magnetoelectronic be hot topics in the research on the magnetics. Along with the rapid decrease of the size, the properties of the semiconductor devices will be influenced by the quantum effects. Diluted magnetic semiconductors (DMSs) can obtain the ferromagnetism (FM) at room temperature by doping magnetic atoms into semiconductor. However, the effect of the magnetic doping is different and even contradict, so the origin of FM is still in debate, such as in zinc oxide (ZnO) [1–3]. After Dietl et al. [4] reported that transition-metal (TM)-doped ZnO would show room temperature ferromagnetism (RTFM), many studies have successively proven that TM doping into ZnO is an effective method to form DMSs. However, because of the debate of the origin of magnetism of TM-doped ZnO, caused by the defects or metal dopants, it is the main hinder in realizing RTFM of ZnO materials. It is well known that the lattice defects include oxygen vacancy (O_V), zinc interstitial, Zn vacancy, as well as interstitial oxygen, which attract extensive research interest from experimental and computational perspective [5–9]. The lattice defects and magnetic cations of substitutional Mn^{2+} have been considered as the main sources of FM of Mn-doped ZnO materials [10–16].

Moreover, many studies also reported that FM in ZnO materials might be from the defects on Zn and O sites, and different fabrication method can induce different defects in ZnO [7,14,17]. Furthermore, the concentration of O_V shows the consistent change with the FM in ZnO, which suggests

*Corresponding author (email: xwzhao@rs.kagu.tus.ac.jp)

that the FM is caused by the O_V [5].

In this paper, the Mn-doped ZnO thin films had been fabricated by rf magnetron sputtering and subsequent anneal process. The influence of anneal condition on the magnetism of the Mn-doped ZnO thin films was investigated. With annealing at 300°C for 30 min, the Mn-doped ZnO thin films clearly demonstrate FM. The relationship between the origin of FM in the Mn-doped ZnO thin films and O_V, as well as Mn^{2+} is discussed.

2 Experimental

2.1 Fabrication of Mn-doped ZnO thin films

Firstly, the Mn-doped ZnO thin films formed on Al_2O_3 substrate had been fabricated by rf magnetron sputtering. The target was with a composite of ZnO and Mn_2O_3 (10 wt%). The base pressure was lower than 5×10^{-4} Pa. The depositing conditions of temperature, working pressure and sputtering power were kept at 300°C, 0.67 Pa and 75 W, respectively. The depositing process had been carried out in the high purity Ar (5N) atmosphere, with the flow rate of 10 mL/cm^3. The presputtering was executed for 5 min to remove possible surface contamination on the target surface. The formed Mn-doped ZnO thin films have been named as "MZO-as". Then, the MZO sample was annealed in O_2 atmosphere at the flow rate of 5 mL/cm^3. The anneal processes are at 300°C, 500°C and 700°C for 3 min, and at 300°C for 3, 30, 50 min, and named as "MZO-*x*°C*y*min".

2.2 Characterization

The crystalline of the MZO thin films was investigated using an X-ray diffraction (XRD, Rigaku Ultima IV) equipped with Cu-Kα radiation (40 kV, 40 mA), employing a scanning rate of 0.01° s^{-1}. The spectra of O 1s and Mn 2p were conducted by X-ray photoelectron spectroscopy (XPS, Jeol JPS-9010MC). Magnetic properties of the samples were carried out using a superconducting quantum interference device (SQUID, Quantum Design MPMS-XL) magnetometry.

3 Results and discussion

3.1 Effect of anneal temperature on MZO thin films

3.1.1 Crystal structure of MZO-x°C3min

The XRD patterns of the MZO-*x*°C3min samples are shown in Figure 1. Besides the peak of Al_2O_3 from substrate, the diffraction peak from the MZO-*x*°C3min samples is around 34.4°, due to the (002) crystal plane of ZnO (JCPDS # 36-1451), corresponding to a wurtzite ZnO structure. Compared with that of MZO-as, it could be clearly found that the peak from (002) crystal plane of the MZO-300°C3min sample becomes stronger after annealing at 300°C for 3 min, indicating a better crystalline structure of ZnO [18,19]. However, with further increasing the anneal temperature to 500°C and 700°C, the intensity of the peak slightly varies, which means that the influence of the anneal temperature over 300°C on crystalline of Mn-doped ZnO is slight.

3.1.2 Magnetism of MZO-x°C3min

Magnetization versus applied magnetic field (*M-H*) curves measured at 5 K by SQUID for the MZO-*x*°C3min samples are shown in Figure 2, where the applied field is parallel to the samples. It can be clearly seen that only the MZO-300°C3min sample exhibits slight ferromagnetic behavior, and other samples might be with antimagnetic behavior. It hints that the ferromagnetic behavior is not only related with the crystalline structure of the MZO thin films.

3.1.3 Bonding environment of MZO-x°C3min

The origin of FM of TM-doped ZnO materials has been usually considered to the concentration of O_V providing

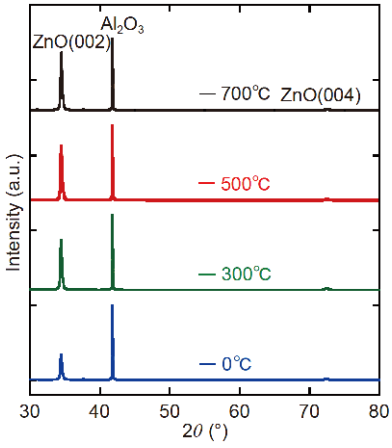

Figure 1 (Color online) XRD patterns of the MZO-*x*°C3min samples.

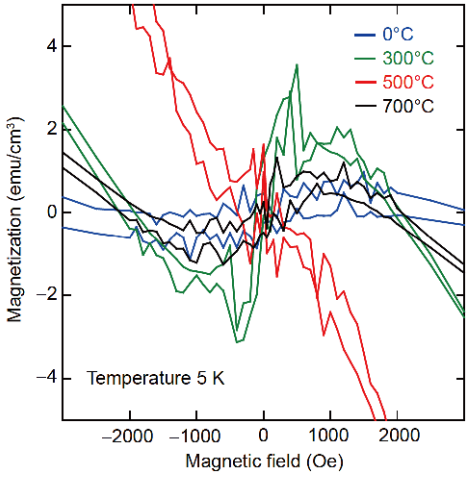

Figure 2 (Color online) *M-H* curves of the MZO-*x*°C3min samples.

more carriers, and the magnetic cations of substitutional Mn^{2+} [4,10,20–22].

In order to further investigate the origin of FM in the MZO thin films, XPS spectra have been used to gain insight into the chemical bonding of the MZO thin films, as shown in Figure 3. The O 1s peaks of the MZO thin films are asymmetric and each peak could yield two contributions due to different chemical states of oxygen, as shown in Figure 3(a). Among them, the peak at 529.5 eV is well known to the O^{2-} ions, normally (lattice oxygen, O_L) in ZnO structure [23,24]. The peak at 531.5 eV could be considered to the oxygen-deficient regions (such as oxygen vacancies, O_V) within the metal oxide matrix and on the surface [24,25]. The relationship between the chemical states of oxygens in the MZO thin films is investigated by the relative area ratios (%) estimated from the fitted curves as displayed in Figure 3(b). Notably, it shows that the O_V obviously decreased from around 55% of that of MZO-as to around 45% of that of MZO-300°C3min, then to around 30% of that with higher anneal temperature, indicating that the O_V decreases and the crystalline increases.

Furthermore, from the Figure 3(c) and (d), it can be clearly found that the relative concentration of Mn^{2+} of the MZO-*x*°C3min samples decreases with increasing the anneal temperature. Considering the result of ferromagnetic behavior from the MZO-300°C3min sample, it could conclude that the complex (O_V + Mn^{2+}) plays the role in inducing the magnetism behavior of the MZO thin films.

3.2 Effect of anneal time on MZO thin films

3.2.1 Crystal structure of MZO-300°Cymin

Based on the above results of anneal temperature on MZO thin films, the effect of anneal time at 300°C had been carried out. Figure 4 shows the XRD patterns of the MZO thin films, with extending the anneal time from 3 to 50 min at 300°C. Compared with that of MZO-300°C3min, it could be clearly found that the peak change of (002) crystal plane is slight with extending the anneal time, until 50 min. In other words, the crystalline of MZO decreases with too long anneal time in O_2 atmosphere.

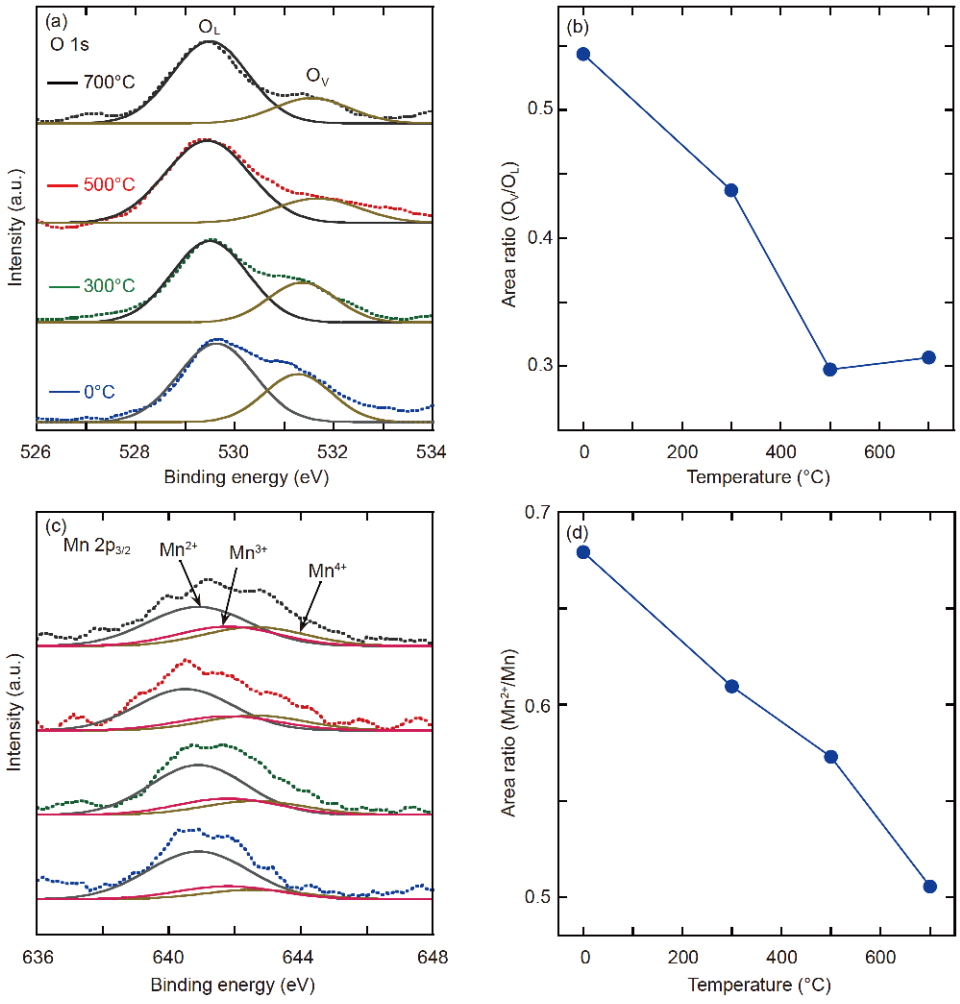

Figure 3 (Color online) XPS spectra of the MZO-*x*°C3min samples. (a) O 1s and (b) its area ratio; (c) Mn 2p and (b) its area ratio. O_L (lattice oxygen), O_V (oxygen vacancy).

3.2.2 *Magnetism of MZO-300°Cymin*

Figure 5 shows the *M-H* curves of the MZO-300°C*y*min samples. With extending the anneal time, the change of the magnetic behavior of the MZO-300°C*y*min samples is obvious (Figure 5(a)). Compared with that of MZO-300°C3min, when the anneal time extends to 30 min, the sample clearly exhibits the ferromagnetic behavior, and the maximum *Ms* around 7 emu/cm^3 is observed in Figure 5(b). Considering the crystalline of MZO-300°C*y*min, it means that the influence of the crystalline structure on the magnetic behavior is important.

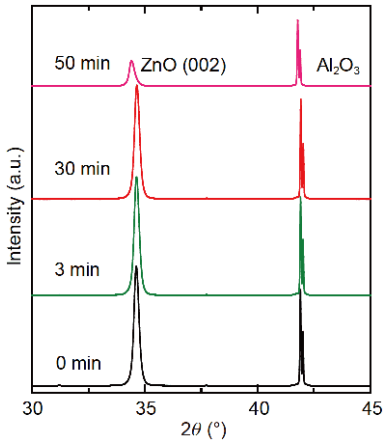

Figure 4 (Color online) XRD patterns of the MZO-300°C*y*min samples.

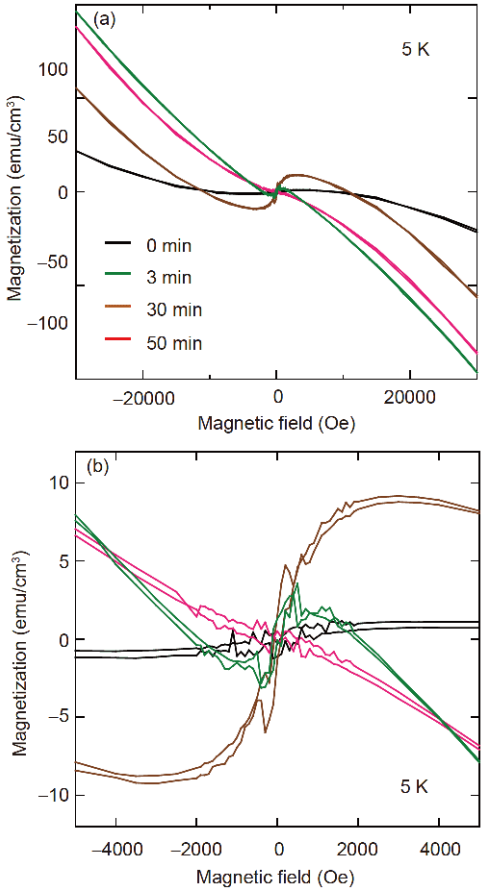

Figure 5 (Color online) *M-H* curves of the MZO-300°C*y*min samples.

3.2.3 *Bonding environment of MZO-300°Cymin*

Figure 6 shows the O 1s peaks of the MZO-300°C*y*min samples. With extending the anneal time to 30 min, the change on the relative area ratios of O_V is obvious, while longer than 30 min, the decrease of O_V becomes slightly, as shown in Figure 6(b). In other words, the O_V of the MZO-300°C30min sample is not the lowest, indicating that the concentration of O_V is not the main role on the ferromagnetic behavior. From Figure 7, it can be clearly found that the relative concentration of Mn^{2+} of the MZO-300°C*y*min samples first increases then decreases, with extending the anneal time. Furthermore, the relative concentration of Mn^{2+} shows relatively higher in the MZO-300°C3min and MZO-300°C30min samples. Compared with that of the relative concentration O_V and substitutional Mn^{2+} on ferromagnetic behavior, it could conclude that O_V plays the main role in inducing the FM of the MZO thin films with good crystal structure.

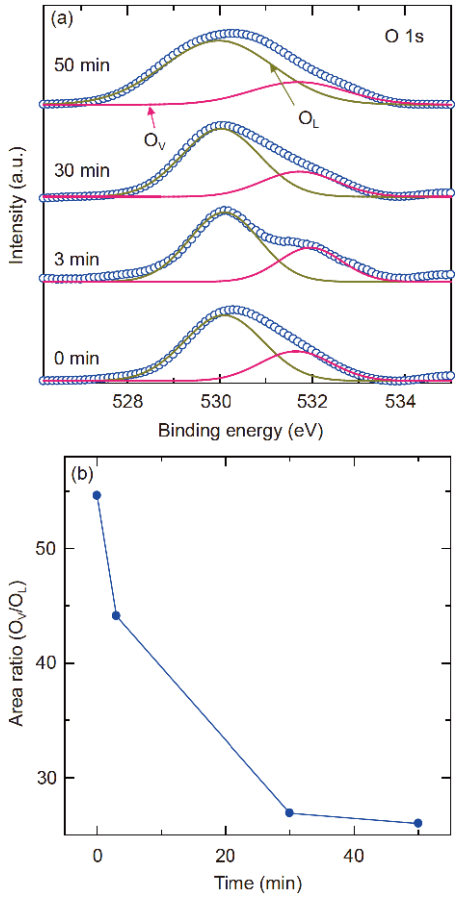

Figure 6 (Color online) XPS spectra of the MZO-300°C*y*min samples. (a) O 1s and (b) its area ratio.

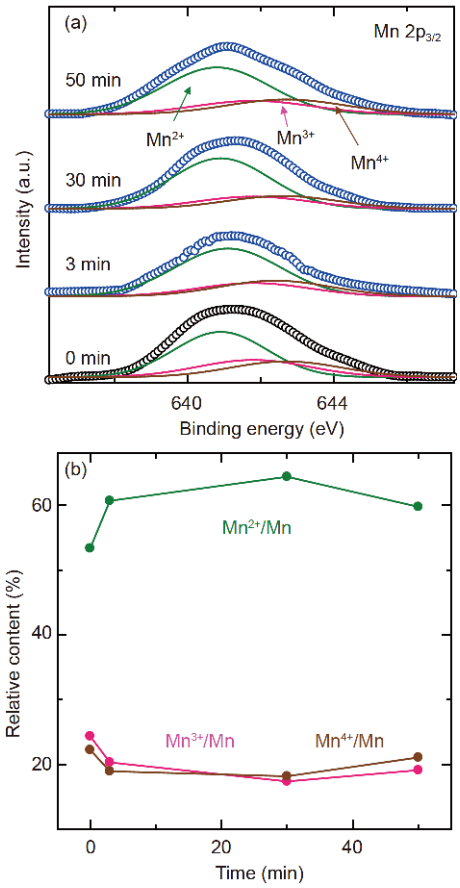

Figure 7 (Color online) XPS spectra of the MZO-300°C*y*min samples. (a) Mn 2p and (b) its area ratio.

4 Conclusion

In summary, Mn-doped ZnO thin films with ferromagnetic behavior had been successfully fabricated by rf magnetron sputtering and subsequent anneal process. The influence of anneal temperature from 300°C to 700°C for 3 min on the magnetism of the Mn-doped ZnO thin films is slight. While extending the anneal time from 3 to 30 min at 300°C, the Mn-doped ZnO thin films obviously demonstrate FM. Compared with the effect of O_V and substitutional Mn^{2+} on magnetic behavior, O_V plays the main role in inducing FM of the Mn-doped ZnO thin films with good crystal structure.

1 Ando K. Materials science: Seeking room-temperature ferromagnetic semiconductors. Science, 2006, 312: 1883–1885
2 Chen B, Yu Q X, Gao Q Q, et al. Structural reconstruction and defects transition in mediating room temperature ferromagnetism in Co-doped ZnO film. Appl Phys Lett, 2013, 102: 132405
3 Garcia M A, Merino J M, Fernández Pinel E, et al. Magnetic properties of ZnO nanoparticles. Nano Lett, 2007, 7: 1489–1494
4 Dietl T, Ohno H, Matsukura F, et al. Zener model description of ferromagnetism in zinc-blende magnetic semiconductors. Science, 2000, 287: 1019–1022
5 Wang Q, Sun Q, Chen G, et al. Vacancy-induced magnetism in ZnO thin films and nanowires. Phys Rev B, 2008, 77: 205411
6 Lee J K, Nastasi M, Hamby D W, et al. Optical observation of donor-bound excitons in hydrogen-implanted ZnO. Appl Phys Lett, 2005, 86: 171102
7 Tuomisto F, Ranki V, Saarinen K, et al. Evidence of the Zn vacancy acting as the dominant acceptor in n-type ZnO. Phys Rev Lett, 2003, 91: 205502
8 Cui Y, Shi S, Chen L, et al. Hydrogen-doping induced reduction in the phase transition temperature of VO_2: A first-principles study. Phys Chem Chem Phys, 2015, 17: 20998–21004
9 Shi S, Gao J, Liu Y, et al. Multi-scale computation methods: Their applications in lithium-ion battery research and development. Chin Phys B, 2016, 25: 018212
10 Qi B, Ólafsson S, Gíslason H P. Vacancy defect-induced d0 ferromagnetism in undoped ZnO nanostructures: Controversial origin and challenges. Prog Mater Sci, 2017, 90: 45–74
11 Rainey K, Chess J, Eixenberger J, et al. Defect induced ferromagnetism in undoped ZnO nanoparticles. J Appl Phys, 2014, 115: 17D727
12 Snure M, Kumar D, Tiwari A. Ferromagnetism in Ni-doped ZnO films: Extrinsic or intrinsic? Appl Phys Lett, 2009, 94: 012510
13 Ahmed Khan Z, Ghosh S. Robust room temperature ferromagnetism in Cu doped ZnO thin films. Appl Phys Lett, 2009, 99: 042504
14 Ilyas U, Rawat R S, Wang Y, et al. Alteration of Mn exchange coupling by oxygen interstitials in ZnO:Mn thin films. Appl Surf Sci, 2012, 258: 6373–6378
15 Sasikala Devi A A, Roqan I S. Analysis on the energetics, magnetism and electronic properties in a 45° ZnO grain boundary doped with Gd. RSC Adv, 2018, 8: 13850–13856
16 Sharma P, Gupta A, Rao K V, et al. Ferromagnetism above room temperature in bulk and transparent thin films of Mn-doped ZnO. Nat Mater, 2003, 2: 673–677
17 Djerdj I, Jaglicić Z, Arcon D, et al. Co-doped ZnO nanoparticles: Minireview. Nanoscale, 2010, 2: 1096–1104
18 Gao W, Li Z. ZnO thin films produced by magnetron sputtering. Ceramics Int, 2004, 30: 1155–1159
19 Kim C, Kim S, Lee C. Effects of rf power and substrate temperature during rf magnetron sputtering on crystal quality of zno thin films. Jpn J Appl Phys, 2005, 44: 8501–8503
20 Yan H, Wang J, Zhong X, et al. Spatial distribution of manganese and room temperature ferromagnetism in manganese-doped ZnO nanorods. Appl Phys Lett, 2008, 19: 142502
21 Ando K, Saito H, Jin Z, et al. Magneto-optical properties of ZnO-based diluted magnetic semiconductors. J Appl Phys, 2001, 89: 7284–7286
22 Chattopadhyay S, Neogi S K, Sarkar A, et al. Defects induced ferromagnetism in Mn doped ZnO. J Magn Magn Mater, 2011, 323: 363–368
23 Chen S, Carraro G, Barreca D, et al. Aerosol assisted chemical vapour deposition of Ga-doped ZnO films for energy efficient glazing: Effects of doping concentration on the film growth behaviour and opto-electronic properties. J Mater Chem A, 2015, 3: 13039–13049
24 Bekermann D, Gasparotto A, Barreca D, et al. Highly oriented ZnO nanorod arrays by a novel plasma chemical vapor deposition process. Cryst Growth Des, 2010, 10: 2011–2018
25 Sahai A, Goswami N. Probing the dominance of interstitial oxygen defects in ZnO nanoparticles through structural and optical characterizations. Ceramics Int, 2014, 40: 14569–14578